

# Non-Adiabatic Reaction Dynamics in the Gas-Phase Formation of Phosphinidenesilylene, the Isovalent Counterpart of Hydrogen Isocyanide, under Single-Collision Conditions

Chao He, Zhenghai Yang, Srinivas Doddipatla, Long Zhao, Shane Goettl, Ralf I. Kaiser,\* Mateus Xavier Silva, and Breno R. L. Galvão\*



Cite This: *J. Phys. Chem. Lett.* 2021, 12, 2489–2495



Read Online

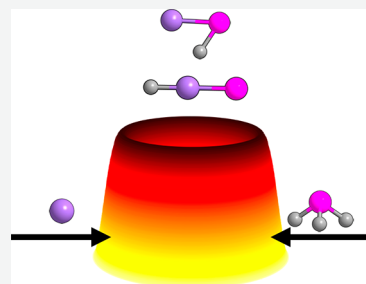
ACCESS |

Metrics & More

Article Recommendations

Supporting Information

**ABSTRACT:** The phosphinidenesilylene ( $\text{HPSi}; \text{X}^1\text{A}'$ ) molecule was prepared via a directed gas-phase synthesis in the bimolecular reaction of ground-state atomic silicon ( $\text{Si}; {}^3\text{P}$ ) with phosphine ( $\text{PH}_3; \text{X}^1\text{A}_1$ ) under single-collision conditions. The chemical dynamics are initiated on the triplet surface via addition of a silicon atom to the non-bonding electron pair of phosphine, followed by non-adiabatic dynamics and surface hopping to the singlet manifold, accompanied by isomerization via atomic hydrogen shift and decomposition to phosphinidenesilylene ( $\text{HPSi}, \text{X}^1\text{A}'$ ) along with molecular hydrogen. Statistical calculations predict that silylidynephosphine ( $\text{HSiP}, \text{X}^1\Sigma^+$ ) is also formed, albeit with lower yields. The barrier-less route to phosphinidenesilylene opens up a multipurpose mechanism to access the hitherto obscure class of phosphasilylenes through silicon–phosphorus coupling via reactions of atomic silicon with alkylphosphines under single-collision conditions in the absence of successive reactions of the reaction products, which are not feasible to prepare by traditional synthetic routes.



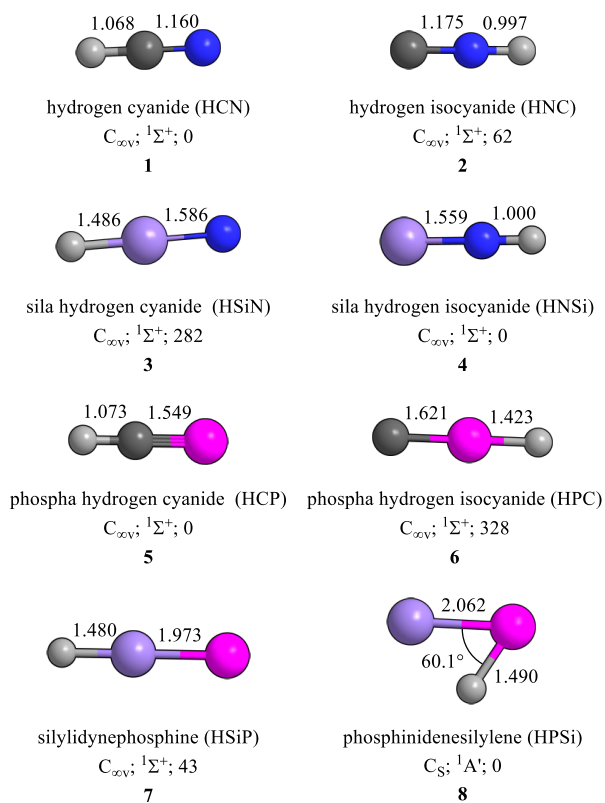
Since the pioneering isolation of hydrogen cyanide ( $\text{HCN}, \text{X}^1\Sigma^+, \mathbf{1}$ ) from Prussian Blue ( $\text{Fe}_4[\text{Fe}(\text{CN})_6]$ ) by the Swedish chemist Carl Wilhelm Scheele in 1782,<sup>1</sup> the structural isomer hydrogen isocyanide ( $\text{HNC}, \text{X}^1\Sigma^+, \mathbf{2}$ )<sup>2–7</sup> and the isovalent homologues sila hydrogen cyanide ( $\text{HSiN}, \text{X}^1\Sigma^+, \mathbf{3}$ ), sila hydrogen isocyanide ( $\text{HNSi}, \text{X}^1\Sigma^+, \mathbf{4}$ ), phospha hydrogen cyanide ( $\text{HCP}, \text{X}^1\Sigma^+, \mathbf{5}$ ), phospha hydrogen isocyanide ( $\text{HPC}, \text{X}^1\Sigma^+, \mathbf{6}$ ), silylidynephosphine ( $\text{HSiP}, \text{X}^1\Sigma^+, \mathbf{7}$ ), and phosphinidenesilylene ( $\text{HPSi}, \text{X}^1\text{A}', \mathbf{8}$ ) have fascinated the physical (organic), inorganic, material, astrochemistry, and theoretical chemistry communities from the fundamental points of views of electronic structure and chemical bonding (Scheme 1).<sup>8,9</sup> These molecules are considered as prototypes of highly reactive hydrides, in which the light, second-row main group XIV and XV elements—carbon and nitrogen—are substituted by their third-row isovalent atoms—silicon and phosphorus.<sup>10</sup> Whereas for the isoelectronic isomer pair of  $\text{HNC}$ – $\text{HCN}$ ,  $\mathbf{1}$  is thermodynamically favored by  $62 \text{ kJ mol}^{-1}$  than its isomer  $\mathbf{2}$ ,<sup>11</sup> the trend is reversed when a carbon atom is replaced by an isovalent group XIV silicon atom: sila hydrogen isocyanide ( $\text{HNSi}, \mathbf{4}$ ) is calculated to be thermodynamically more stable by  $282 \text{ kJ mol}^{-1}$  compared to the sila hydrogen cyanide isomer ( $\text{HSiN}, \mathbf{3}$ ),<sup>11,12</sup> with both isomers discovered in rare gas matrices.<sup>13,14</sup> The formal replacement of nitrogen in  $\mathbf{1}$  and  $\mathbf{2}$  by the main group XV element phosphorus leads to phospha hydrogen cyanide ( $\text{HCP}, \mathbf{5}$ ) and phospha hydrogen isocyanide ( $\text{HPC}, \mathbf{6}$ ) with the latter isomer being thermodynamically less stable by  $328 \text{ kJ mol}^{-1}$ , considering, e.g., the weak H–P bond compared to the stronger H–C bond in  $\mathbf{5}$ . Similar to  $\mathbf{1}$ ,<sup>2</sup>  $\mathbf{5}$  was

detected in the circumstellar envelope of the Asymptotic Giant Branch (AGB) carbon-rich star IRC+10216 via four rotational transitions.<sup>15,16</sup> In analogy to  $\mathbf{2}$ , one may expect the thermodynamically less stable isomer  $\mathbf{6}$  to be abundant in deep space; however, this species has eluded any laboratory and astronomical detection to date. The silylidynephosphine ( $\text{HSiP}, \mathbf{7}$ ) and phosphinidenesilylene ( $\text{HPSi}, \mathbf{8}$ ) species represent a peculiar, scarcely studied isomer pair.  $\mathbf{8}$  was first identified in the gas phase through the discharge of silane ( $\text{SiH}_4$ )–phosphine ( $\text{PH}_3$ ) mixtures via rotational spectroscopy.<sup>17</sup> Whereas  $\mathbf{1}$ – $\mathbf{7}$  are linear and hold a  $C_{\infty v}$  point groups,<sup>11,18</sup> quantum chemical calculations suggest that  $\mathbf{8}$  adopts an exotic bent structure bearing a P=Si double bond, a P–H single bond, and a donor–acceptor interaction between the P–H bond and the empty p orbital at the silicon atom.<sup>11,17–20</sup> This chemical bonding favors  $\mathbf{8}$  compared to the linear isomer  $\mathbf{7}$  by  $43 \text{ kJ mol}^{-1}$ ; a transition state involving a hydrogen shift for the  $\mathbf{7} \rightarrow \mathbf{8}$  isomerization is located  $54 \text{ kJ mol}^{-1}$  above  $\mathbf{7}$ .<sup>21</sup> Nevertheless, any directed gas-phase synthesis on phosphinidenesilylene ( $\text{HPSi}, \mathbf{8}$ ) along with its alkyl-substituted derivatives has remained elusive as of this date.

Received: January 9, 2021

Accepted: February 18, 2021

**Scheme 1. Molecular Geometries of Isovalent Species of Hydrogen Cyanide (HCN) and Hydrogen Isocyanide (HNC), Including the Relative Energies (kJ mol<sup>-1</sup>), Bond Distances (Å), and Selected Bond Angles<sup>a</sup>**



<sup>a</sup>Atoms are colored as follows: carbon, black; silicon, purple; nitrogen, blue; hydrogen, gray; and phosphorus, pink.

Herein, we provide an exceptional glance into the unknown chemistry of phosphinidenesilylene (HPSi, 8) and report the very first *directed* gas-phase preparation of 8 under single-collision conditions through the bimolecular reaction of atomic silicon (Si; <sup>3</sup>P) with phosphine (PH<sub>3</sub>; X<sup>1</sup>A<sub>1</sub>) utilizing the crossed molecular beams techniques. An investigation at the most fundamental, microscopic level combined with electronic structure calculations provides a unique look into the exotic reaction mechanisms and non-adiabatic reaction dynamics through which highly reactive phosphorus–silicon molecules like 8 are prepared as a result of a single collision between the simplest open-shell silicon-bearing species (atomic silicon) and the prototype closed-shell phosphorus-bearing molecule (phosphine). The chemical dynamics of the reaction involve an addition of atomic silicon to the non-bonding electron pair of phosphine in the entrance channel on the triplet surface, non-adiabatic dynamics via surface hopping from the triplet to the singlet manifold, isomerization of the singlet intermediate via hydrogen migration, and the formation of phosphinidenesilylene (HPSi, 8) via molecular hydrogen loss. These findings illuminate exotic silicon–phosphorus chemistry and bond coupling along with unusual chemical dynamics of silicon, which are quite distinct from those of the isovalent carbon system.<sup>22,23</sup>

The crossed molecular beams reaction of electronically ground-state silicon atoms (Si; <sup>3</sup>P) with phosphine (PH<sub>3</sub>; X<sup>1</sup>A<sub>1</sub>) was carried out under single-collision conditions in a crossed molecular beam machine by intersecting supersonic

beams of atomic silicon (Si; <sup>3</sup>P) and phosphine (PH<sub>3</sub>; X<sup>1</sup>A<sub>1</sub>) at 90°, resulting in a collision energy (E<sub>C</sub>) of 11.9 kJ mol<sup>-1</sup>. The neutral reaction products were ionized through electron impact at 80 eV within a triply differentially pumped quadrupole mass spectrometry (QMS) detector and then mass- and velocity-analyzed to record angular resolved time-of-flight (TOF) spectra.<sup>24</sup> In this operation mode, QMS transmits an ion of a univocal mass-to-charge (*m/z*) ratio, while the detector records the arrival time of this ion after a reactive collision and ionization of the neutral product. According to the isotopes of silicon (<sup>28</sup>Si, 92.23%; <sup>29</sup>Si, 4.67%; <sup>30</sup>Si, 3.10%) and phosphorus (<sup>31</sup>P, 100%), a reactive scattering signal for the ground-state silicon atoms (Si)–phosphine (PH<sub>3</sub>) reaction was collected at *m/z* from 64 to 59. This accounts for potential adducts (<sup>30</sup>SiPH<sub>3</sub><sup>+</sup>, *m/z* = 64; <sup>29</sup>SiPH<sub>3</sub><sup>+</sup>, *m/z* = 63; <sup>28</sup>SiPH<sub>3</sub><sup>+</sup>, *m/z* = 62) together with products corresponding to the emission of atomic (<sup>30</sup>SiPH<sub>2</sub><sup>+</sup>, *m/z* = 63; <sup>29</sup>SiPH<sub>2</sub><sup>+</sup>, *m/z* = 62; <sup>28</sup>SiPH<sub>2</sub><sup>+</sup>, *m/z* = 61) and molecular hydrogen (<sup>30</sup>SiPH<sup>+</sup>, *m/z* = 62; <sup>29</sup>SiPH<sup>+</sup>, *m/z* = 61; <sup>28</sup>SiPH<sup>+</sup>, *m/z* = 60) and to the fragments formed upon dissociative electron impact ionization (<sup>30</sup>SiP<sup>+</sup>, *m/z* = 61; <sup>29</sup>SiP<sup>+</sup>, *m/z* = 60; <sup>28</sup>SiP<sup>+</sup>, *m/z* = 59). No signal was observed at *m/z* = 64, 63, and—within the error limits of 3 ± 3%—at *m/z* = 62, suggesting the absence of any adducts. Ion counts at *m/z* = 61 and 59 were accumulated at a proportion of 7 ± 3% and 27 ± 3% compared with *m/z* = 60. These time-of-flight (TOF) spectra are identical after scaling; along with the isotopic substitution pattern, this finding suggests the existence of a single reaction channel, i.e., the reaction of ground-state atomic silicon with phosphine forming HSiP isomer(s)—predominantly via the reaction of <sup>28</sup>Si—along with the emission of molecular hydrogen (H<sub>2</sub>; 2 amu) leading to signal at *m/z* = 60 (H<sup>28</sup>SiP; hereafter: HSiP). The signals at *m/z* = 62 and 61 originate from reactions of <sup>30</sup>Si and <sup>29</sup>Si with phosphine, whereas the signal at *m/z* = 59 stems from dissociative electron impact ionization of the parent molecules. Consequently, the laboratory data suggest that the reaction of ground-state silicon atoms with phosphine involves the formation of HPSi isomer(s) via the atomic silicon versus the molecular hydrogen exchange pathway. Corresponding TOF spectra and the full laboratory angular distributions were accumulated at *m/z* = 60 (Figure 1). This distribution is rather broad, almost forward–backward symmetric with regard to the center-of-mass (CM) angle of 46.3° (Table S1), and distributes a scattering of angles from at least 11.3° to 66.3°. These results indicate that the reaction proceeds via indirect scattering dynamics involving the existence of SiPH<sub>3</sub> intermediate(s) that ultimately undergo(es) unimolecular decomposition via molecular hydrogen loss.<sup>25</sup>

Our ultimate goal is to explore the nature of the HPSi isomer(s) along with the underlying reaction mechanism(s) on the pertinent SiPH<sub>3</sub> potential energy surface(s) (PESSs), accessed through the crossed molecular beams reaction of ground-state silicon atoms (Si; <sup>3</sup>P) with phosphine (PH<sub>3</sub>; X<sup>1</sup>A<sub>1</sub>). To achieve these objectives, a forward convolution of the laboratory data into the CM reference frame is crucial. This procedure fits the laboratory data (Figure 1) and yields the CM translational energy *P*(E<sub>T</sub>) and angular *T*(θ) flux distributions (Figure 2).<sup>26</sup> Within our error limits, the best-fit CM functions were achieved with a single channel of the product mass combination of 60 amu (HPSi) and 2 amu (H<sub>2</sub>). The resulting *P*(E<sub>T</sub>) distribution reveals a maximum translational energy release (*E*<sub>max</sub>) of 196 ± 16 kJ mol<sup>-1</sup>. Considering the energy conservation, the maximum translational energy

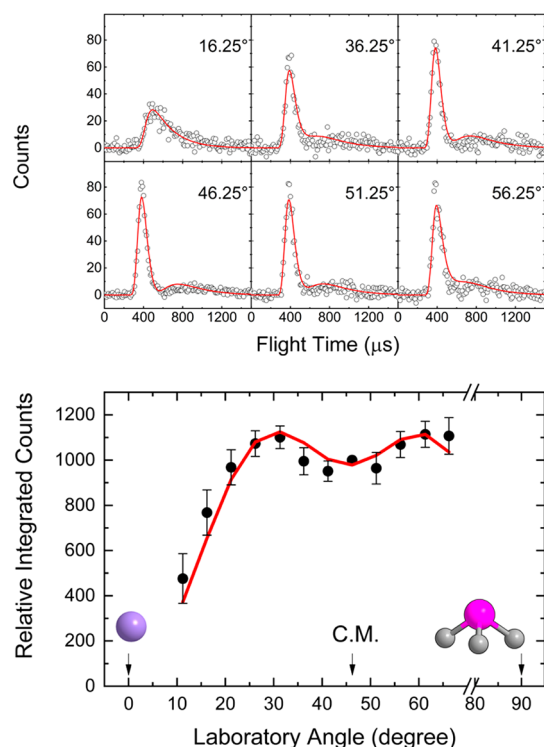


**Figure 1.** TOF spectra (top) and laboratory angular distribution (bottom) collected at  $m/z$  60 for the reaction of silicon ( $\text{Si}; ^3\text{P}$ ) with phosphine ( $\text{PH}_3; \text{X}^1\text{A}_1$ ). The black circles represent the experimental data, while the red lines define the best fits.

( $E_{\max}$ ), the collision energy ( $E_C = 11.9 \pm 0.2 \text{ kJ mol}^{-1}$ ), and the reaction energy ( $\Delta_r G$ ) are communicated through  $E_{\max} = E_C -$

$\Delta_r G$  toward the molecules born without rovibrational excitation. Therefore, the reaction is calculated to be exoergic by  $184 \pm 16 \text{ kJ mol}^{-1}$ . Furthermore, the  $P(E_T)$  distribution peaked well away from zero translational energy at  $80 \pm 7 \text{ kJ mol}^{-1}$ , suggesting a tight exit transition state with a repulsive energy release and significant “reorganization” of the electron density from the decomposing complex to the final products.<sup>25</sup> Further, the average translational energy of the products was derived to be  $87 \pm 7 \text{ kJ mol}^{-1}$ , indicating that  $44 \pm 4\%$  of the available energy is transformed into the translational degrees of freedom of the products. Finally,  $T(\theta)$  depicts non-zero intensity over the complete scattering range from  $0^\circ$  to  $180^\circ$ ; this finding is indicative of indirect scattering dynamics via the formation of  $\text{SiPH}_3$  complex(es); the forward–backward symmetry of  $T(\theta)$  implies that the lifetime of the decomposing  $\text{SiPH}_3$  complex is longer than the rotational period(s).<sup>27</sup>

We now merge our experimental results with the computational data to untangle the underlying reaction mechanism(s) of the reaction of the silicon atoms ( $\text{Si}; ^3\text{P}$ ) with phosphine ( $\text{PH}_3; \text{X}^1\text{A}_1$ ) (Figure 3, Figures S1 and S2, and Tables S2 and S3). The electronic structure calculations indicate the formation of four distinct HPSi isomers, **p1–p4**, that can be produced via molecular hydrogen emission: singlet phosphinidenesilylene (**p1**,  $\text{X}^1\text{A}'$ ,  $\Delta_r G = -159 \pm 10 \text{ kJ mol}^{-1}$ ), singlet silylidynephosphine (**p2**,  $\text{X}^1\Sigma^+$ ,  $\Delta_r G = -114 \pm 10 \text{ kJ mol}^{-1}$ ), triplet silylidynephosphine (**p3**,  $\text{X}^3\text{A}'$ ,  $\Delta_r G = 9 \pm 10 \text{ kJ mol}^{-1}$ ), and triplet phosphinidenesilylene (**p4**,  $\text{X}^3\text{A}''$ ,  $\Delta_r G = 28 \pm 10 \text{ kJ mol}^{-1}$ ). A comparison of these data with the experimentally calculated reaction energy of  $\Delta_r G = -184 \pm 16 \text{ kJ mol}^{-1}$  reveals the formation of at least singlet phosphinidenesilylene (**p1**). Formation of the higher energy isomers **p2** and/or **p3** cannot be excluded at this stage, since these might be hidden in the low-energy section of the translational energy

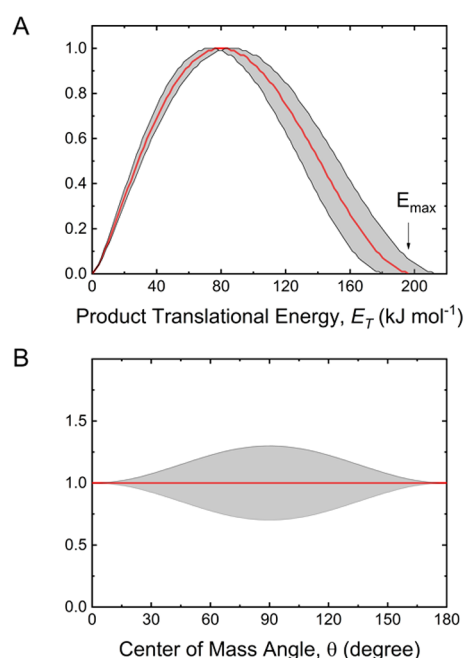


**Figure 2.** CM translational energy flux distribution (A), CM angular flux distribution (B), and the top view of the corresponding flux contour map (C) leading to the formation of silylidynephosphine ( $\text{HSiP}$ ) and phosphinidenesilylene ( $\text{HPSi}$ ) plus molecular hydrogen in the atomic silicon ( $\text{Si}; ^3\text{P}$ ) with phosphine ( $\text{PH}_3; \text{X}^1\text{A}_1$ ) system. Shaded areas indicate the acceptable upper and lower error limits, while the red solid lines define the best fits. The flux contour map represents the flux intensity of the reactively scattered heavy products as a function of the CM scattering angle ( $\theta$ ) and product velocity ( $u$ ). The color bar manifests the flux gradient from high (H) intensity to low (L) intensity. Colors of the atoms: silicon, purple; phosphorus, pink; and hydrogen, gray.

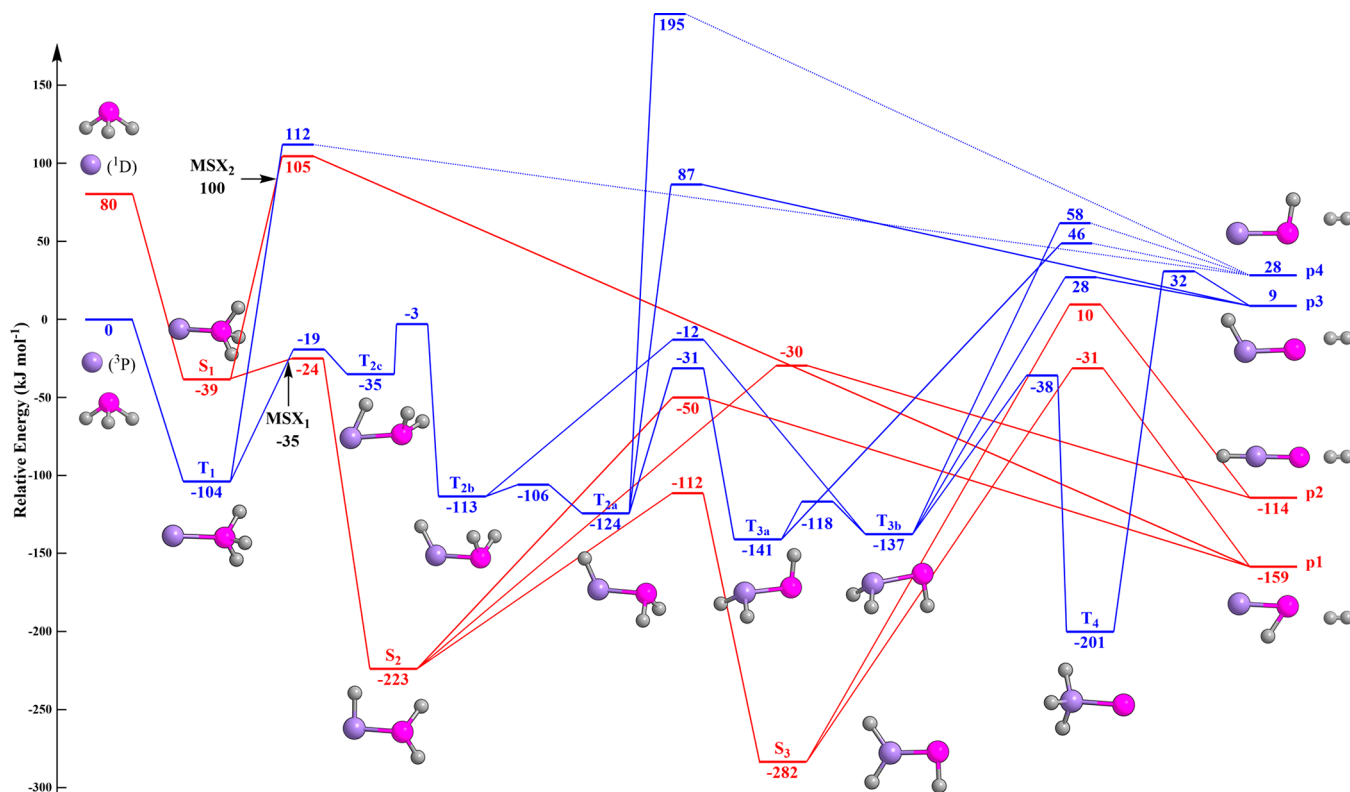


**Figure 3.** Potential energy diagram of the reaction of atomic silicon (Si;  ${}^3\text{P}/{}^1\text{D}$ ) with phosphine ( $\text{PH}_3$ ;  $\text{X}^1\text{A}_1$ ) calculated at the CCSD(T)-F12/aug-cc-pV(T+d)Z//M06-2X/cc-pV(T+d)Z+ZPE(M06-2X/cc-pV(T+d)Z) level of theory. The energies are shown in  $\text{kJ mol}^{-1}$  with respect to the energy of the separated reactants. Atoms are colored as follows: silicon, purple; hydrogen, gray; and phosphorus, pink. Cartesian coordinates and normal modes are compiled in Tables S3.

distribution. If only **p2** or **p3** is formed, the resulting translation energy distributions would terminate near 126 or 3  $\text{kJ mol}^{-1}$ , which would be inconsistent with our experimental results. Note that our calculations also explored possible atomic hydrogen loss channels leading to  $\text{SiPH}_2$  isomers (Figure S1): silylenephosphino (**p5**,  ${}^2\text{A}'$ ,  $\Delta_r G = 72 \pm 10 \text{ kJ mol}^{-1}$ ), *trans*-phosphinidenesilyl (**p6**,  ${}^2\text{A}'$ ,  $\Delta_r G = 92 \pm 10 \text{ kJ mol}^{-1}$ ), phosphinosilylidene (**p7**,  ${}^2\text{A}''$ ,  $\Delta_r G = 104 \pm 10 \text{ kJ mol}^{-1}$ ), and *cis*-phosphinidenesilyl (**p8**,  ${}^2\text{A}'$ ,  $\Delta_r G = 108 \pm 10 \text{ kJ mol}^{-1}$ ). However, taking into account the collision energy in our study of 11.9  $\text{kJ mol}^{-1}$ , the formation of **p4**–**p8** is ruled out since the reaction endoergicities cannot be compensated by our collision energy. Recall that the absence of atomic hydrogen loss was also established experimentally. Overall, we can conclude that our data support at least the formation of singlet phosphinidenesilylene (**p1**) under single-collision conditions. Considering the  ${}^1\text{A}_1$  and  ${}^3\text{P}$  electronic ground states of the phosphine and silicon reactants and the  ${}^1\text{A}'$  and  ${}^1\Sigma_g^+$  states of singlet phosphinidenesilylene (**p1**) and molecular hydrogen, non-adiabatic reaction dynamics involving inter-system crossing (ISC) from the triplet to the singlet manifold must be involved in the formation of singlet phosphinidenesilylene (**p1**).

The unraveling of non-adiabatic reaction dynamics necessitates the exploration of the triplet and singlet  $\text{SiPH}_3$  PESs. These computations located seven triplet and three singlet  $\text{SiPH}_3$  intermediates ( $\text{S}_1$ – $\text{S}_3$ ,  $\text{T}_1$ ,  $\text{T}_{2a}$ ,  $\text{T}_{2b}$ ,  $\text{T}_{2c}$ ,  $\text{T}_{3b}$ ,  $\text{T}_4$ ), 21 transition states, and two singlet–triplet seam of crossings (MSX<sub>1</sub>, MSX<sub>2</sub>). The reaction is initiated on the triplet surface via a barrierless addition of the ground-state silicon (Si;  ${}^3\text{P}$ ) to

the non-bonding electron pair of the phosphorus atom of phosphine, leading to a  $\text{C}_s$ -symmetric triplet phosphoranylenesilylene ( $\text{SiPH}_3$ ,  $\text{T}_1$ ,  ${}^3\text{A}''$ ) intermediate. A hydrogen atom migration connects  $\text{T}_1$  to phosphinosilylene ( $\text{HSiPH}_2$ ,  $\text{T}_{2c}$ ,  $\text{C}_s$ ,  ${}^3\text{A}''$ ), which can then isomerize to its *cis* form ( $\text{HSiPH}_2$ ,  $\text{T}_{2b}$ ,  $\text{C}_s$ ,  ${}^3\text{A}''$ ) and *trans*-phosphinosilylene ( $\text{HSiPH}_2$ ,  $\text{T}_{2a}$ ,  $\text{C}_s$ ,  ${}^3\text{A}''$ ). Alternatively,  $\text{T}_{2a}$  and  $\text{T}_{2b}$  can undergo further isomerization via hydrogen shifts, yielding *trans/cis*-silylene-phosphine ( $\text{H}_2\text{SiPH}$ ,  $\text{T}_{3a}$ / $\text{T}_{3b}$ ,  $\text{C}_s$ ,  ${}^3\text{A}''$ ). Yet another hydrogen migration from the PH group to the  $\text{SiH}_2$  moiety in  $\text{T}_{3b}$  yields silylphosphinidene ( $\text{H}_3\text{SiP}$ ,  $\text{T}_4$ ,  $\text{C}_s$ ,  ${}^3\text{A}''$ ). With the exception of the molecular hydrogen loss from  $\text{T}_{3b}$  to **p4**, all molecular hydrogen loss pathways are closed since the exit transition states are higher in energy than the collision energy and hence energetically not accessible.

On the singlet surface, the calculations identified three intermediates:  $\text{S}_1$ – $\text{S}_3$ .  $\text{S}_1$  ( $\text{SiPH}_3$ ,  $\text{C}_s$ ,  ${}^1\text{A}'$ ) represents the singlet analogue of  $\text{T}_1$  and isomerizes via a hydrogen shift to phosphinosilylene ( $\text{HSiPH}_2$ ,  $\text{S}_2$ ,  $\text{C}_s$ ,  ${}^1\text{A}'$ ) through a barrier of only 15  $\text{kJ mol}^{-1}$ .  $\text{S}_2$  may also proceed via an atomic hydrogen migration, leading to the global minimum of the  $\text{SiPH}_3$  surface: silylenephosphine ( $\text{H}_2\text{SiPH}$ ,  $\text{S}_3$ ,  $\text{C}_s$ ,  ${}^1\text{A}'$ ). Our computations identified four energetically accessible and tight molecular hydrogen loss channels—two from each intermediate  $\text{S}_2$  and  $\text{S}_3$ —leading to singlet phosphinidenesilylene ( $\text{HPSi}$ , **p1**,  $\text{C}_s$ ,  $\text{X}^1\text{A}'$ ) and singlet silylidynephosphine ( $\text{HSiP}$ , **p2**,  $\text{C}_{\text{oo}}$ ,  $\text{X}^1\Sigma^+$ ). In order to evaluate the possibility of ISC between the triplet and singlet manifolds, minima on the seam-of-crossings (MSX) were searched for and identified (MSX<sub>1</sub> and MSX<sub>2</sub>). MSX<sub>1</sub> is located in the vicinity of the isomerization path of intermediate  $\text{T}_1$  to  $\text{T}_{2a}$  prior to passing the transition state, crosses the

isomerization of  $S_1$  to  $S_2$ , and shows a spin–orbit coupling (SOC) of  $63\text{ cm}^{-1}$ .  $\text{MSX}_2$  is located in the vicinity of  $S_1/\text{T}_1$  decomposition, with a SOC of  $54\text{ cm}^{-1}$ . The reaction pathway starts with  $\text{T}_1$ , but before arriving at the transition state for the molecular hydrogen emission on the triplet surface, the singlet and triplet states cross. At the transition state, the singlet surface is lower in energy than the triplet manifold. However, considering  $E_C = 11.9\text{ kJ mol}^{-1}$  under our experimental conditions,  $\text{MSX}_2$  cannot be accessed; hence, the reaction must proceed via  $\text{MSX}_1$  (Figure 4). Based on these considerations,

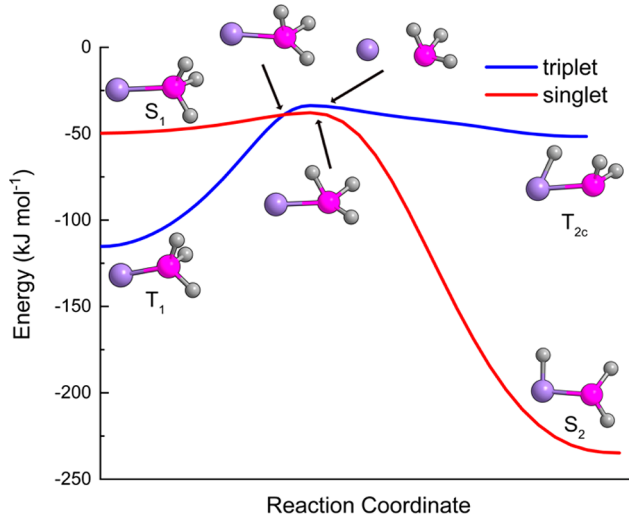


**Figure 4.** Results of intrinsic reaction coordinate (IRC) calculations at the M06-2X/cc-pV(T+d)Z level of theory showing the singlet–triplet crossing involved in the first hydrogen-atom migration isomerization. The geometry of the fully optimized  $\text{MSX}_1$  lies in the vicinity of these paths. The reaction coordinate is a mass-weighted internal coordinate, scaled for an improved visualization.

we propose that the reaction is initiated on the triplet surface via the barrierless addition of ground-state atomic silicon to the non-bonding electron pair of the phosphorus atom of phosphine, yielding the triplet phosphoranylidenesilylene intermediate ( $\text{SiPH}_3$ ,  $\text{T}_1$ ,  $^3\text{A}''$ ). The latter undergoes ISC via  $\text{MSX}_1$  in conjunction with hydrogen migration to singlet phosphino silylene ( $\text{HSiPH}_2$ ,  $\text{S}_2$ ,  $\text{C}_s$ ,  $^1\text{A}'$ ) (Figure 4), which may then process unimolecular decomposition through  $\text{H}_2$  molecule loss to yield phosphinidene silylene ( $\text{HPSi}$ ,  $\text{p1}$ ,  $\text{X}^1\text{A}'$ ) via a tight exit transition state. Alternatively,  $\text{S}_2$  isomerizes via a hydrogen shift to silylene phosphine ( $\text{H}_2\text{SiPH}$ ,  $\text{S}_3$ ,  $\text{C}_s$ ,  $^1\text{A}'$ ), which then emits molecular hydrogen to form the experimentally detected phosphinidenesilylene ( $\text{HPSi}$ ,  $\text{p1}$ ,  $\text{X}^1\text{A}'$ ). Note that, in principle, both  $\text{S}_2$  and  $\text{S}_3$  may also emit molecular hydrogen, yielding the thermodynamically less stable singlet, silylidynephosphine ( $\text{HSiP}$ ,  $\text{p2}$ ,  $\text{C}_{\infty\nu}$ ,  $\text{X}^1\text{\Sigma}^+$ ).

To elucidate the possible contributions of singlet silylidynephosphine ( $\text{HSiP}$ ,  $\text{p2}$ ,  $\text{C}_{\infty\nu}$ ,  $\text{X}^1\text{\Sigma}^+$ ), Rice–Ramsperger–Kassel–Marcus (RRKM) theory was exploited to predict the branching ratios of  $\text{p1}$  and  $\text{p2}$  under the premise of a complete energy randomization in the decomposing intermediates(s) on the singlet surface (Table S2).<sup>28,29</sup> These studies reveal that phosphinidenesilylene ( $\text{HPSi}$ ,  $\text{p1}$ ,  $\text{X}^1\text{A}'$ ) and silylidynephosphine ( $\text{HSiP}$ ,  $\text{p2}$ ,  $\text{X}^1\text{\Sigma}^+$ ) contribute close to 67% and 33% at  $E_C = 11.9\text{ kJ mol}^{-1}$ , respectively. For the main product phosphinidenesilylene ( $\text{HPSi}$ ,  $\text{p1}$ ,  $\text{X}^1\text{A}'$ ), dissociation from  $\text{S}_2$  and  $\text{S}_3$  supplies 53% and 13%, respectively, whereas for

silylidynephosphine ( $\text{HSiP}$ ,  $\text{p2}$ ,  $\text{X}^1\text{\Sigma}^+$ ), decomposition from intermediate  $\text{S}_2$  and  $\text{S}_3$  supplies 33% and 1% at most. Therefore, we may conclude that a hydrogen shift from  $\text{S}_2$  to  $\text{S}_3$  contributes a low proportion in the reaction mechanism. Hence, RRKM calculations and experimental results match well, predicting a dominant formation of phosphinidenesilylene ( $\text{HPSi}$ ,  $\text{p1}$ ,  $\text{X}^1\text{A}'$ ), while RRKM also proposes a non-negligible fraction of silylidynephosphine ( $\text{HSiP}$ ,  $\text{p2}$ ,  $\text{X}^1\text{\Sigma}^+$ ).

In conclusion, merging crossed molecular beams and computational study on the bimolecular reaction of silicon atoms with phosphine under single-collision conditions revealed a facile gas-phase preparation of phosphinidenesilylene ( $\text{HPSi}$ ,  $\text{p1}$ ,  $\text{X}^1\text{A}'$ ). The chemical dynamics are initiated on the triplet surface via addition of a silicon atom to the non-bonding electron pair of phosphine in the entrance channel, followed by surface hopping from the triplet to the singlet manifold, accompanied by isomerization via atomic hydrogen shift and unimolecular decomposition of the thermodynamically most stable isomer, phosphinidenesilylene ( $\text{HPSi}$ ,  $\text{p1}$ ,  $\text{X}^1\text{A}'$ ), along with molecular hydrogen. Statistical calculations predict that the silylidynephosphine ( $\text{HSiP}$ ,  $\text{p2}$ ,  $\text{X}^1\text{\Sigma}^+$ ) is also formed, albeit with lower yields. Considering that these isomers have dipole moments of  $10.53\text{ D}$  and  $12.11\text{ D}$ ,<sup>32</sup> our studies suggest that both isomers are potential candidates for searches in circumstellar envelopes of IRC+10216 and toward star-forming regions like SgrB2, where phosphine has been detected.<sup>30</sup> The barrier-less route to phosphinidenesilylene ( $\text{HPSi}$ ,  $\text{p1}$ ,  $\text{X}^1\text{A}'$ ) via the crossed molecular beams reaction of the ground-state silicon atoms with phosphine can be taken as a benchmark to synthesize even more complex, hitherto elusive substituted phosphorus–silicon compounds, such as phosphasilenes ( $\text{RPSi}$ ) with R being an organic side chain, in the gas phase by means of a directed synthesis through the reaction of atomic silicon with the corresponding alkylphosphines ( $\text{PH}_2\text{R}$ ). This unconventional route could make it possible to prepare previously rarely investigated organo phosphorus–silicon compounds, which are not easily accessed by classical synthetic methods. Theoretical calculations predicted that the relative stability of  $\text{RSiP}$  (phosphasilynes) versus their constitutional isomers  $\text{RPSi}$  (phosphasilenylidenes) correlates with the electronegativity of the substituent R. Electronegative substituents, such as fluorine (F), the methyl group ( $\text{CH}_3$ ), and the phenyl radical ( $\text{C}_6\text{H}_5$ ), stabilize the  $\text{Si}\equiv\text{P}$  triple bond in phosphasilynes ( $\text{RSiP}$ ), whereas electropositive substituents, such as lithium (Li), beryllium hydride ( $\text{BeH}$ ), borane ( $\text{BH}_2$ ), hydrogen (H), and silyl ( $\text{SiH}_3$ ), favor the bent phosphasilenylidene isomer ( $\text{RPSi}$ ) bearing a  $\text{Si}=\text{P}$  double bond and a lone pair of electrons at silicon.<sup>18,31</sup> For instance, (methylsilylidyne)phosphine ( $\text{H}_3\text{CSi}\equiv\text{P}$ ) is predicted to be more stable than (methylphosphinidene)silylene ( $\text{Si}=\text{PCH}_3$ ) by  $23\text{ kJ mol}^{-1}$ , which was calculated utilizing the CCSD(T) level. The barrier for a 1,2- $\text{CH}_3$  shift of (methylsilylidyne)phosphine ( $\text{H}_3\text{CSi}\equiv\text{P}$ ) is about  $105\text{ kJ mol}^{-1}$ , whereas a barrier height of  $84\text{ kJ mol}^{-1}$  is estimated for the reverse process.<sup>18</sup> Therefore, if  $\text{H}_3\text{CSi}\equiv\text{P}$  and/or  $\text{Si}=\text{PCH}_3$  were synthesized in molecular beam experiments, they would not interconvert. In this way, molecular beam experiments are of particular advantage to prepare elusive phosphinidenesilylenes, since in these studies, the primary reaction products do not undergo any consecutive reactions after their gas-phase formation such as dimerization since they “fly away” unperturbed.

## ASSOCIATED CONTENT

### Supporting Information

The Supporting Information is available free of charge at <https://pubs.acs.org/doi/10.1021/acs.jpcllett.1c00085>.

Experimental and computational details; Figure S1, schematic representation of reactants and products of the reaction of atomic silicon with phosphine leading to p1–p8; Figure S2, schematic representation of the potential energy surface of the reaction of atomic silicon with phosphine; Table S1, peak velocities and speed ratios of the silicon and phosphine beams along with the corresponding collision energy and center-of-mass angle; Table S2, statistical branching ratios for the reaction of the silicon atom with phosphine; and Table S3, optimized Cartesian coordinates and vibrational frequencies for the reaction of atomic silicon with phosphine (PDF)

## AUTHOR INFORMATION

### Corresponding Authors

**Ralf I. Kaiser** — Department of Chemistry, University of Hawai'i at Manoa, Honolulu, Hawaii 96822, United States;  [0000-0002-7233-7206](https://orcid.org/0000-0002-7233-7206); Email: [ralfk@hawaii.edu](mailto:ralfk@hawaii.edu)

**Breno R. L. Galvão** — Centro Federal de Educação Tecnológica de Minas Gerais, CEFET-MG, 30421-169 Belo Horizonte, Minas Gerais, Brazil;  [0000-0002-4184-2437](https://orcid.org/0000-0002-4184-2437); Email: [brenogalvao@gmail.com](mailto:brenogalvao@gmail.com)

### Authors

**Chao He** — Department of Chemistry, University of Hawai'i at Manoa, Honolulu, Hawaii 96822, United States

**Zhenghai Yang** — Department of Chemistry, University of Hawai'i at Manoa, Honolulu, Hawaii 96822, United States

**Srinivas Doddipatla** — Department of Chemistry, University of Hawai'i at Manoa, Honolulu, Hawaii 96822, United States

**Long Zhao** — Department of Chemistry, University of Hawai'i at Manoa, Honolulu, Hawaii 96822, United States

**Shane Goettl** — Department of Chemistry, University of Hawai'i at Manoa, Honolulu, Hawaii 96822, United States

**Mateus Xavier Silva** — Centro Federal de Educação Tecnológica de Minas Gerais, CEFET-MG, 30421-169 Belo Horizonte, Minas Gerais, Brazil

Complete contact information is available at: <https://pubs.acs.org/10.1021/acs.jpcllett.1c00085>

### Notes

The authors declare no competing financial interest.

## ACKNOWLEDGMENTS

This experimental work was supported by the U.S. National Science Foundation (NSF) under Award CHE-1853541 to the University of Hawaii. Financial support from Coordenação de Aperfeiçoamento de Pessoal de Nível Superior — Brasil (CAPES), Finance Code 001, and Conselho Nacional de Desenvolvimento Científico e Tecnológico (CNPq) is also acknowledged.

## REFERENCES

- Scheele, C. W. Über die farbende Materie in Berlinerblau. *Neue Schwed. Akadem. Abhandl.* **1782**, 3, 256–266.
- Snyder, L. E.; Buhl, D. Observations of Radio Emission from Interstellar Hydrogen Cyanide. *Astrophys. J.* **1971**, 163, L47–L52.
- Blackman, G. L.; Brown, R. D.; Godfrey, P. D.; Gunn, H. I. The Microwave Spectrum of HNC: Identification of U90. 7. *Nature* **1976**, 261, 395–396.
- Snyder, L. E.; Buhl, D. Detection of Several New Interstellar Molecules. *Ann. N. Y. Acad. Sci.* **1972**, 194, 17–24.
- Zuckerman, B.; Morris, M.; Palmer, P.; Turner, B. E. Observations of CS, HCN, U89. 2, and U90. 7 in NGC 2264. *Astrophys. J.* **1972**, 173, L125–L129.
- Milligan, D. E.; Jacox, M. E. Infrared Spectroscopic Evidence for the Species HNC\*. *J. Chem. Phys.* **1963**, 39, 712–715.
- Creswell, R. A.; Pearson, E. F.; Winnewisser, M.; Winnewisser, G. Detection of the Millimeter Wave Spectrum of Hydrogen Isocyanide, HNC<sup>1,2</sup>. *Z. Naturforsch., A: Phys. Sci.* **1976**, 31, 221–224.
- Baudler, M. Chain and Ring Phosphorus Compounds—Analogies between Phosphorus and Carbon Chemistry. *Angew. Chem., Int. Ed. Engl.* **1982**, 21, 492–512.
- Kaiser, R. I.; Mebel, A. M. On the Formation of Polyacetylenes and Cyanopolyacetylenes in Titan's Atmosphere and Their Role in Astrobiology. *Chem. Soc. Rev.* **2012**, 41, 5490–5501.
- Parker, D. S. N.; Mebel, A. M.; Kaiser, R. I. The Role of Isovalency in the Reactions of the Cyano (CN), Boron Monoxide (BO), Silicon Nitride (SiN), and Ethynyl (C<sub>2</sub>H) Radicals with Unsaturated Hydrocarbons Acetylene (C<sub>2</sub>H<sub>2</sub>) and Ethylene (C<sub>2</sub>H<sub>4</sub>). *Chem. Soc. Rev.* **2014**, 43, 2701–2713.
- Devarajan, D.; Frenking, G. Are They Linear, Bent, or Cyclic? Quantum Chemical Investigation of the Heavier Group 14 and Group 15 Homologues of HCN and HNC. *Chem. - Asian J.* **2012**, 7, 1296–1311.
- Kroto, H. W.; Murrell, J. N.; Al-Derzi, A.; Guest, M. F. Calculated Structures and Microwave Frequencies of HNSi and HSiN. *Astrophys. J.* **1978**, 219, 886–890.
- Ogilvie, J. F.; Cradock, S. Spectroscopic Studies of the Photodecomposition of Silyl Azides in Argon Matrices near 4 K: Detection of Iminosilicon, HNSi. *Chem. Commun.* **1966**, 0, 364–365.
- Maier, G.; Glatthaar, J. Silane Nitrile: Matrix Isolation, Adduct with Hydrogen. *Angew. Chem., Int. Ed. Engl.* **1994**, 33, 473–475.
- Gier, T. E. HCP, A Unique Phosphorus Compound. *J. Am. Chem. Soc.* **1961**, 83, 1769–1770.
- Agúndez, M.; Cernicharo, J.; Guélin, M. Discovery of Phosphaethyne (HCP) in Space: Phosphorus Chemistry in Circumstellar Envelopes. *Astrophys. J.* **2007**, 662, L91–L94.
- Lattanzi, V.; Thorwirth, S.; Halfen, D. T.; Mück, L. A.; Ziurys, L. M.; Thaddeus, P.; Gauss, J.; McCarthy, M. C. Bonding in the Heavy Analogue of Hydrogen Cyanide: the Curious Case of Bridged HPSi. *Angew. Chem., Int. Ed.* **2010**, 49, 5661–5664.
- Lai, C.-H.; Su, M.-D.; Chu, S.-Y. Effects of First-Row Substituents on Silicon-Phosphorus Triple Bonds. *Inorg. Chem.* **2002**, 41, 1320–1322.
- Baboul, A. G.; Schlegel, H. B. Structures and Energetics of Some Silicon - Phosphorus Compounds: SiH<sub>m</sub>PH<sub>n</sub>, SiH<sub>m</sub>PH<sub>n</sub>SiH<sub>o</sub>, and (SiH<sub>3</sub>)<sub>3</sub>P. An ab Initio Molecular Orbital Study. *J. Am. Chem. Soc.* **1996**, 118, 8444–8451.
- Zachariah, M. R.; Melius, C. F. Theoretical Calculation of Thermochemistry for Molecules in the Si-P-H System. *J. Phys. Chem. A* **1997**, 101, 913–918.
- Chesnut, D. B. A Topographical Study of Bonding in the PP and SiP Hydrides. *Chem. Phys.* **2005**, 315, 59–64.
- Guo, Y.; Gu, X.; Zhang, F.; Sun, B. J.; Tsai, M. F.; Chang, A. H. H.; Kaiser, R. I. Unraveling the Formation of HCPH (X<sup>2</sup>A') Molecules in Extraterrestrial Environments: Crossed Molecular Beam Study of the Reaction of Carbon Atoms, C(<sup>3</sup>P<sub>1</sub>), with Phosphine, PH<sub>3</sub>(X<sup>1</sup>A<sub>1</sub>). *J. Phys. Chem. A* **2007**, 111, 3241–3247.
- Rey-Villaverde, R.; Alvarez-Barcia, S.; Flores, J. R. The Dynamics of the C + PH<sub>3</sub> Reaction: A Theoretical Study. *J. Chem. Phys.* **2012**, 137, 014316.

(24) Gu, X.; Kaiser, R. I. Reaction Dynamics of Phenyl Radicals in Extreme Environments: a Crossed Molecular Beam Study. *Acc. Chem. Res.* **2009**, *42*, 290–302.

(25) Levine, R. D. *Molecular Reaction Dynamics*; Cambridge University Press: Cambridge, 2005.

(26) Kaiser, R. I.; Lee, Y. T.; Suits, A. G. Crossed-beam Reaction of Carbon Atoms with Hydrocarbon Molecules. I. Chemical Dynamics of the Propargyl Radical Formation,  $C_3H_3$  ( $X^2B_2$ ), from Reaction of  $C(^3P_1)$  with Ethylene,  $C_2H_4$  ( $X^1A_g$ ). *J. Chem. Phys.* **1996**, *105*, 8705–8720.

(27) Miller, W. B.; Safron, S. A.; Herschbach, D. R. Exchange Reactions of Alkali Atoms with Alkali Halides: a Collision Complex Mechanism. *Discuss. Faraday Soc.* **1967**, *44*, 108–122.

(28) Steinfeld, J. I.; Francisco, J. S.; Hase, W. L. *Chemical Kinetics and Dynamics*; Prentice Hall: Englewood Cliffs, NJ, 1982.

(29) Kislov, V. V.; Nguyen, T. L.; Mebel, A. M.; Lin, S. H.; Smith, S. C. Photodissociation of Benzene under Collision-Free Conditions: An Ab Initio/Rice-Ramsperger-Kassel-Marcus Study. *J. Chem. Phys.* **2004**, *120*, 7008–7017.

(30) Agúndez, M.; Cernicharo, J.; Decin, L.; Encrenaz, P.; Teyssier, D. Confirmation of Circumstellar Phosphine. *Astrophys. J., Lett.* **2014**, *790*, L27.

(31) Driess, M.; Monsé, C.; Bläser, D.; Boese, R.; Bornemann, H.; Kuhn, A.; Sander, W. Synthesis and Molecular Structure of Fluoro(triphosphanyl)silane and Attempts to Synthesize a Silyli-dyne-Phosphane. *J. Organomet. Chem.* **2003**, *686*, 294–305.

(32) Bruna, P. J.; Dohmann, H.; Peyerimhoff, S. D. Multireference (Single) and Double-Excitation – Configuration Interaction (MRD-CI) Study of the Radicals CN, SiN, and SiP, and the Linear Structures of HSiP and SiPH in Their Electronic Ground and Various Excited States. *Can. J. Phys.* **1984**, *62*, 1508–1523.